International Journal of Applied Engineering & Technology

FUZZY LOGIC CONTROL OF A 400 KV TRANSMISSION LINE BY A STATCOM BASED ON NPC MULTILEVEL VOLTAGE INVERTERS

Leila Boukarana[1], Sid Ali Fellag[2] and Idir Habi[3]
[13]Faculty of Hydrocarbons and Chemistry, University of M'Hamed Bougara - Boumerdes.
[2]Faculty of Engineering Sciences, University of M'Hamed Bougara - Boumerdes.
[3]LREEI, (Research Laboratory on the Electrification of Industrial Companies) at the Faculty of Hydrocarbons and Chemistry, University of M'Hamed Bougara - Boumerdes.
[1]l.boukarana@univ-boumerdes.dz , [2]s.fellag@univ-boumerdes.dz and [3]h.idir@univ-boumerdes.dz

ABSTRACT
Recent developments in power systems mean that it will be increasingly difficult to reliably control power transfers in highly interconnected systems using traditional slow response time control systems such as phase-shifting transformers and passives shunts or series compensators.

This has recently led to studies of a new generation of FACTS (Flexible AC Transmission System) control devices, using new power static components that can control both opening and closing: a FACTS device.

This paper introduces the STATCOM, a power device reliant on a semiconductor power switches for controlling electrical networks. It serves to enhance the regulation of both active and reactive power transmitted through power lines. Specifically, the STATCOM compensates the reactive energy of the lines, maintains the voltage levels at the bus bars and enables the power source to operate with a unity power factor.

After a concise introduction to the operating principle of the STATCOM, a model is presented featuring key control loops including Phase-Locked Loop (PLL), DC bus voltage control, and power control. Linear controllers (Proportional Integral PI) are used and an approach using Fuzzy Logic Controllers (FLC) is tested. Simulation results for a 400 kV line conducted within the Matlab/Simulink environment are presented, providing a comparative analysis and discussion on the effectiveness of the adopted control strategies in addressing both dynamic and static aspects of the system. Finally, a comparative study between the two approaches (PI and FLC) is conducted and presented.

Keywords: Electrical Network Control, Reactive Energy Compensation, FACTS, STATCOM, NPC Multi-level Inverter, PWM, PLL, Linear Control (PI), Fuzzy Logic Controllers (FLC).

1. INTRODUCTION
All power electronic-based devices aimed at enhancing power system operation are categorized under the FACTS concept. The technology employed in these systems, utilizing static switches, provides them with greater speed compared to traditional electromechanical systems. Additionally, they have the capability to control the power flow within the network, thereby enhancing its effective carrying capacity while simultaneously maintaining or improving network stability. [1].

A concise summary of the impact of using each FACTS to solve the various problems that hinder the smooth operation of the power system is provided in Table (1).

Tab.1: Application of FACTS to Network Problem Solving.

	Load control	Voltage control	Stability Transient	Amplitude of Oscillations
SVC	+	++	+	++
STATCOM	+	+++	+	++
TCSC	++	+	+++	++
SSSC	+ + +	++	+ + +	+ +
UPFC	+ + +	+ + +	+ + +	+ + +
low(+ +) : Medium , (+ + +) : strong				

Transmission lines play a crucial role in electrical networks, consisting of series and shunt impedances. The series impedance can affect the maximum power capacity, while the shunt impedance, predominantly capacitive, influences voltage regulation along the transmission line. Power flow is determined by the series impedance of the line, alongside the input and output voltages of the mains, and the phase difference between these voltages.

FACTS are used to manipulate series and shunt parameters, as well as the phase shift of transmission line voltages, in order to control power flow. [2].

Figure 1: summarizes the influence of the different parts of the UPFC on the power flow.

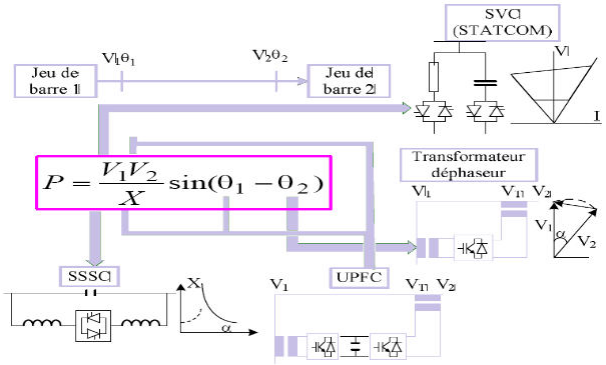

Fig.1: Techniques for active power flow control

The UPFC converter can therefore operate in four modes:

- Voltage regulation.
- Series compensation.
- Phase angle adjustment.
- Automatic mode.

Conventional compensators cannot achieve automatic mode. To demonstrate how the UPFC can influence the power flow in this mode, the UPFC is connected to the starting point S, Figure (2).

The UPFC is represented by two ideal voltage sources. The S and R buses represent the input and the output of the UPFC respectively, [3], [4], [5], [6].

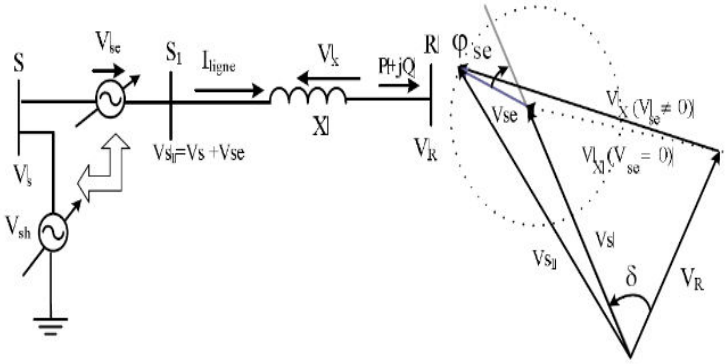

Fig.2: Vector diagram of transmission line with UPFC.

In this paper, an AC transmission system incorporating a STATCOM is investigated The study encompasses the design, identification of references, and control blocks, including the utilization of different controllers (classical PI and fuzzy PI).

2. STATCOM STRUCTURE AND OPERATING PRINCIPLE

A STATCOM is a circuit with a single port connected in parallel with the mains. It utilizes forced switching, with high switching frequencies of the switches. Its energy storage element is a capacitor, forming a DC port.

The main areas of application for the Power Controller include controlling power transits on lines are as follows:

The operation principle of the STATCOM is very similar to that of the synchronous compensator. The output voltages are generated by an inverter rather than a rotating unit.

STATCOM is a circuit with a single port connected in parallel with the mains. It uses forced switching, with high switching frequencies of the switches. Its energy storage element is a capacitor, forming a DC port..

The main areas of application for the Power Controller which controls power transits on lines are as follows:

- Improving the stability of electricity networks.
- Operating equipment and lines at full capacity.
- Interconnecting networks for improving overall grid reliability and resilience.

The exchange of reactive energy is performed by the control of the inverter voltage Vsh, which is in phase with the bus bar voltage Vk=V where the STATCOM is connected.

Figure (3) shows the basic diagram of a STATCOM and its equivalent diagram whose role is to exchange reactive energy with the grid. For this purpose, the inverter is coupled to the grid via a three-phase transformer.

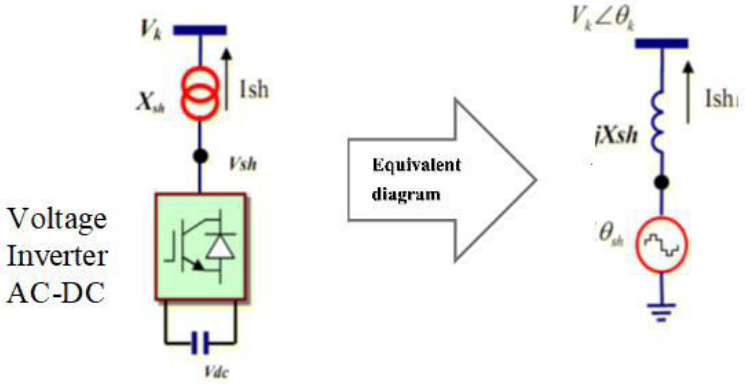

Fig.3: Basic diagram of a STATCOM and the equivalent diagram of a STATCOM

The operation can be described as follows:

The flow of active and reactive powers between these two voltage sources is given by:

$$P = \frac{V_k V_{sh}}{x_{sh}} sin\delta \quad (1)$$

$$Q = \frac{V_k}{V_{sh}}(V_k - V_{sh} cos\delta) \quad (2)$$

From equations (1) and (2) it is evident that when the two voltages are in phase (δ=0), there is only one reactive power flow. The value of the power exchanged depends solely on the amplitudes of the two voltages Vk and Vsh.

There are three possible cases, all considering δ=0:

- **If Vk > Vsh:** An inductive current Ish is established between the two voltage sources through the reactance Xsh, this current is delayed by 90 degrees from Vk, the STATCOM absorbs reactive power from the connection node and consequently the node voltage V1 decreases.

- **If Vk = Vsh:** then Q = 0, signifying that no reactive power is generated or absorbed.
- **If Vk < Vsh**: Since the capacitive current Ish flowing through the choke is 90 degrees ahead of the node voltage, the STATCOM generates reactive power at the connection node, i.e. the node voltage increases, [7].

Figure (4) shows the static characteristic of this converter.

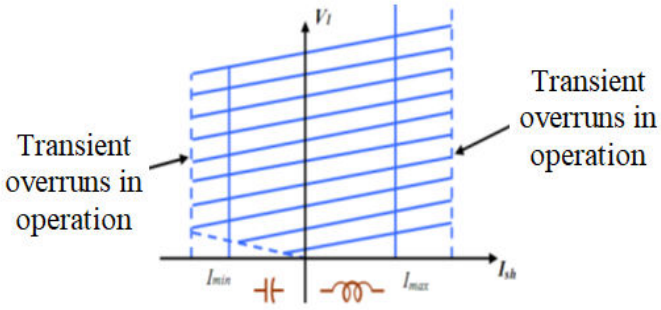

Fig.4: Static characteristics of a STATCOM

3. STATCOM MODELLING

STATCOM is the SVC version, consisting of a high-tech semiconductor-based voltage inverter (IGBT, IGCT) combined with a capacitor as a DC voltage source. They are all connected in parallel to the grid via a coupling transformer, as shown in Figure 4, [8], [9].

The vector relationship between the currents and voltages of a phase on the AC side is expressed by equation (3).

$$\bar{V} - \bar{V}_{sh} = R_{sh}\bar{I}_{sh} + L_{sh}\frac{dI_{sh}}{dt} \quad (3)$$

Or the values are in three-phase:

$$\bar{V} = \begin{bmatrix} V_a \\ V_b \\ V_c \end{bmatrix};\ \bar{V}_{sh} = \begin{bmatrix} V_{ash} \\ V_{bsh} \\ V_{csh} \end{bmatrix};\ I_{sh} = \begin{bmatrix} I_{ash} \\ I_{bsh} \\ I_{csh} \end{bmatrix} \quad (4)$$

When transitioning to the rotating reference frame (d, q), which serves as the synchronism reference frame. We express the STATCOM state system, in matrix form, as follows:

$$\frac{d}{dt}\begin{bmatrix} I_{shd} \\ I_{shq} \end{bmatrix} = \begin{bmatrix} -\frac{R_{sh}}{L_{sh}} & \omega \\ -\omega & -\frac{R_{sh}}{L_{sh}} \end{bmatrix} \cdot \begin{bmatrix} I_{shd} \\ I_{shq} \end{bmatrix} + \frac{1}{L_{sh}}\begin{bmatrix} V_d - V_{shd} \\ V_q - V_{shq} \end{bmatrix} \quad (5)$$

Where the Vector $\begin{bmatrix} V_d - V_{shd} \\ V_q - V_{shq} \end{bmatrix}$ represents the system control vector.

4. STATCOM CONTROL USING CONVENTIONAL PI CONTROLLERS

The main objective of the STATCOM is to compensate the reactive power on the bus bar, thereby ensuring the stability of the bus bar voltage in various practical applications. To achieve this, it injects or absorbs a current Ish*, which represents the reactive the power to be compensated. These currents (Ishd*, Ishq*) serve as the reference variables for the STATOM and are determined based on the required power injection.

5. DC BUS CONTROL

The DC voltage across the capacitor must be kept constant. This necessitates the correction of this voltage by adding an active current to the STATCOM reference current. This active current reflects the active power consumed or supplied by the network. The power exchanged with the capacitor can be expressed by the following equation: [10] [11] [12].

$$P_{dc} = P_{sh} = \frac{1}{2} C \frac{dU_{dc}^2}{dt} => \frac{dU_{dc}^2}{dt} = \frac{2*P_{sh}}{C} \quad (6)$$

If we move to the frequency domain (Laplacian), we get the following:

$$\frac{U_{dc}^2}{P_{sh}} = \frac{2}{C*S} \quad (7)$$

To obtain the P_{sh} signal, we can choose between a proportional and an integral proportional controller. The latter is often preferred because it cancels out the static error [10].

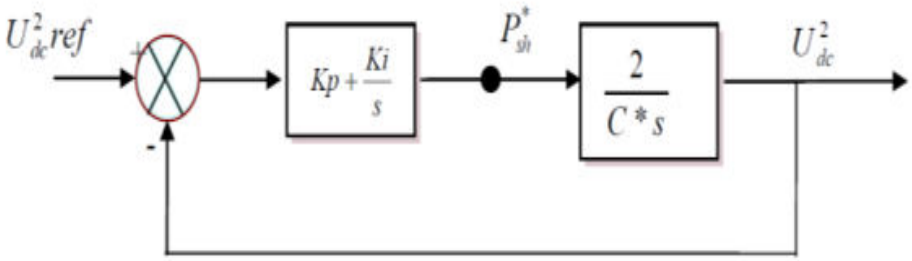

Fig.5: DC voltage regulation.

The closed-loop transfer function of this system in Bode form is given below:

$$F(S) = \frac{U_{dc}^2}{U_{dc-ref}^2} = \frac{\frac{2K_p}{C}S + \frac{2K_i}{C}}{S^2 + \frac{2K_p}{C}S + \frac{2K_i}{C}} \quad (8)$$

With : $\omega_n^2 = \frac{2K_i}{C}$

$$\xi = K_p \sqrt{\frac{1}{2CK_i}} \quad (9)$$

We have selected $\xi = 0.7$ to achieve a favorable control coefficient. Additionally, to dampen fluctuations at 300 Hz and ensure effective filtering, we opt for:

$$\omega_n = \frac{2\pi \times 300}{10} \; rad/sec \quad (10)$$

Finally, the values of $K_P = 0.105$ and $K_i = 10$ are obtained from equation (9).

6. CURRENT (POWER) CONTROL AND REGULATORS SYNTHESIS

The powers injected by the STATCOM are the reactive power Qsh* calculated as a function of the voltage drop, and the active power (Psh* = 0), which represents the joule losses in the DC circuit and the switches in the inverter, [13], [14].

These powers, which are the images of the active and reactive currents (Ishd*, Ishq*), are determined from the following system of equations. These equations are written in the reference frame rotating synchronously (d, q):

$$\begin{bmatrix} I_{shd}^* \\ I_{shq}^* \end{bmatrix} = \frac{2}{3} \frac{1}{V_d^2 + V_q^2} \begin{bmatrix} V_d & -V_q \\ V_q & V_d \end{bmatrix} \cdot \begin{bmatrix} P_{sh}^* \\ Q_{sh}^* \end{bmatrix} \quad (11)$$

Where V_d and V_q are the bus bar voltages. The method of identifying the reference currents can be summarized by the algorithm shown in Figure (6) below:

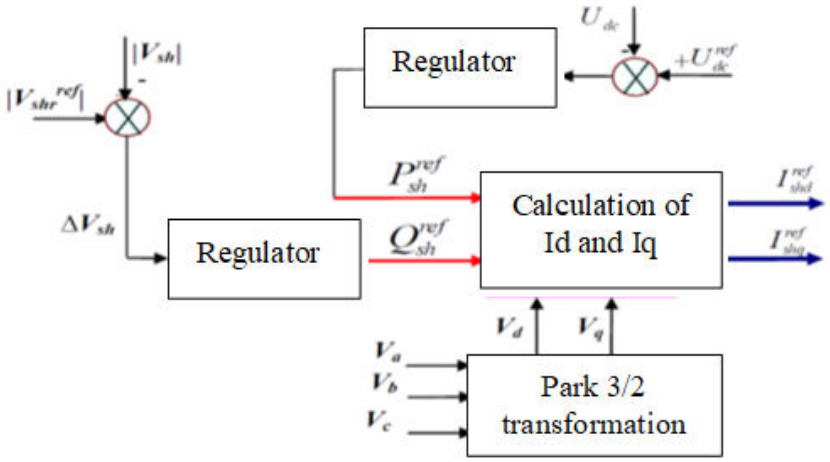

Fig.6: Identification of reference currents.

From the observation, it's evident that there exists a natural coupling in the transfer of the Ishd and Ishq currents. To eliminate this coupling effect, we use the compensation method employing PI regulators to regulate the STATCOM output currents ensuring they closely track their respective Ishd* and Ishq* set points. This is shown in the block diagram in Figure (7).

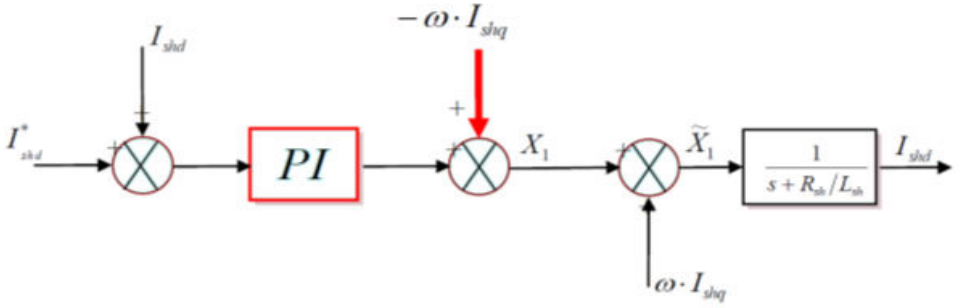

Fig.7: Decoupling control.

In the same way, for the reactive current, we have to add the ω_{Ishd} component and finally arrive at the STATCOM control scheme using the decoupled Watt-Var method shown in Figure (8), [15].

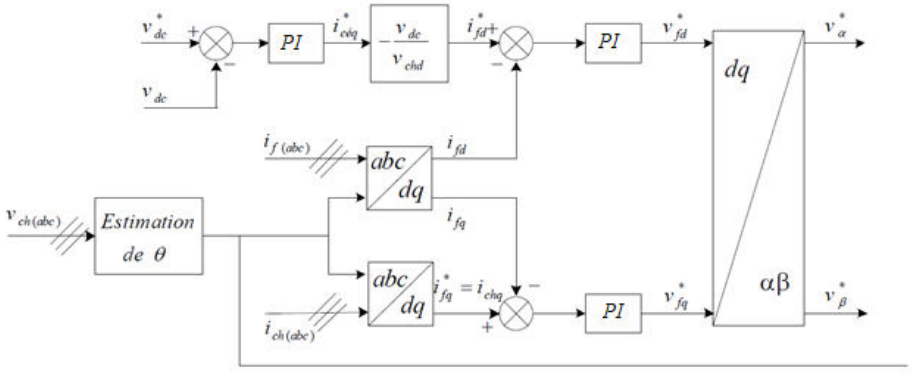

Fig.8: STATCOM regulation diagram.

7. CONTROL OF STATCOM BY A FUZZY LOGIC CONTROLLERS (FLC)

The general principle and the fundamental theory of fuzzy logic include aspects of possibility theory, which involves sets of memberships called fuzzy sets that characterize the various quantities within the system to be controlled. Furthermore, fuzzy reasoning is employed, utilizing a set of fuzzy rules established by human expertise, which can be manipulated to generate the appropriate commands or decisions. Thus, the elements constituting the basic theory of fuzzy logic are [16]:

- Linguistic variables and fuzzy sets.
- Membership functions.
- Operators.
- Fuzzy inferences.

8. DIFFERENT FORMS OF MEMBERSHIP FUNCTIONS

For membership functions, the most common shapes are trapezoidal or triangular. These are the simplest shapes, consisting of pieces of straight lines. The shape is completely defined by 3 points a, b, and c for the triangular shape, or 4 points a, b, c, and d for the trapezoidal one (9).

In most cases, these two shapes are sufficient to delimit fuzzy sets, especially for fuzzy logic control. However, there are other possible shapes, such as the bell shape (Gaussian) and the increasing or decreasing monotone. The rectangular shape is used to represent classical logic [16].

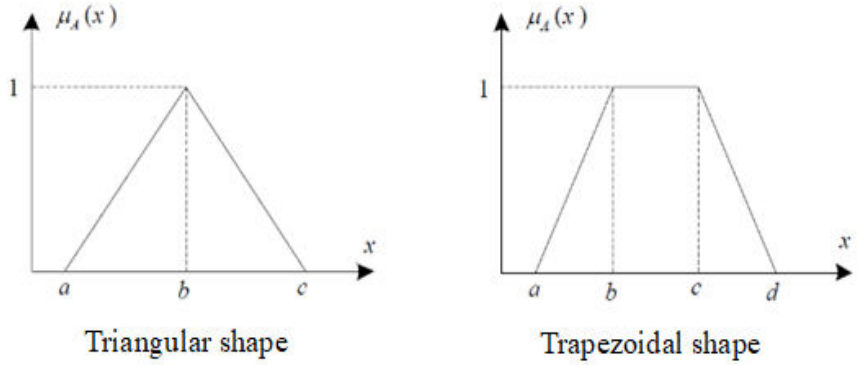

Fig.9: Usual forms of membership functions.

One of the following expressions defines the degree of membership associated with the triangular shape:

$$\mu_A = \begin{cases} \frac{x-a}{b-a} si\ x\epsilon[a,b] \\ \frac{c-x}{c-b} si\ x\epsilon[b,c] \\ 0\ \ si\ x\ is\ elsewhere \end{cases} \quad (12)$$

Or:

$$\mu(x) = max\left(min\left(\frac{x-a}{b-a}, \frac{c-x}{c-b}\right), 0\right) \quad (13)$$

One of the following expressions defines the degree of membership associated with the trapezoid shape:

$$\mu_A = \begin{cases} \frac{x-a}{b-a} si\ x\epsilon[a,b] \\ 1\ \ si\ \ x\epsilon[b,c] \\ \frac{d-x}{d-c} si\ x\epsilon[c,d] \\ 0\ \ si\ \ x\ is\ elsewhere \end{cases} \quad (14)$$

Or:

$$\mu(x) = max\left(min\left(\frac{x-a}{b-a}, \frac{d-x}{d-c}\right), 0\right) \quad (15)$$

It is then possible to associate with linguistic variables coefficients of membership of fuzzy subsets taking values in the interval [0, 1] and quantifying the uncertainty about the variable.

A certain event for the variable will result in a coefficient of membership of the fuzzy subset equal to "1", while the value will be less than "1" in the presence of uncertainty. Consequently, a membership coefficient of zero value signifies complete rejection of the possibility of membership in the selected subset of the variable representing the quantity in question

The universe of discourse of a variable x, denoted by x, representing its domain of variation, can be partitioned into several subsets using membership functions (Ai).

For each value of the variable under consideration, degrees of membership of each fuzzy subset are specified. It's important to note that the membership functions exhibit overlap, which is entirely logical. Indeed, the transition from the fuzzy variable characterized by the membership function A2 to the fuzzy variable characterized by A3 is not abrupt but gradual. This property is of great interest for ensuring the stability of fuzzy logic-based control systems.

9. PRESENTATION OF A FUZZY LOGIC CONTROLLER

The central concept of fuzzy logic control revolves around linguistic control rules. These rules can assume various forms but consistently specify the appropriate control action to undertake in response to a given condition. These command actions may include directives such as "increase the current" or "decrease the voltage significantly", while the conditions might be expressed as "if the voltage error is large enough" or "if the current error is very small". The key words here, such as "big enough", "a lot" and "very small", denote imprecise yet useful information, represented in fuzzy logic theory by fuzzy subsets within a specific universe of discourse. A control rule typically comprises a combination of a condition and an action. Constructing a fuzzy logic controller necessitates multiple rules, which collectively form an algorithm. The general structure of a fuzzy control rule is outlined below.

10. BASIC ELEMENTS OF A FUZZY CONTROLLER

The general diagram of a fuzzy controller is shown in Figure (10):

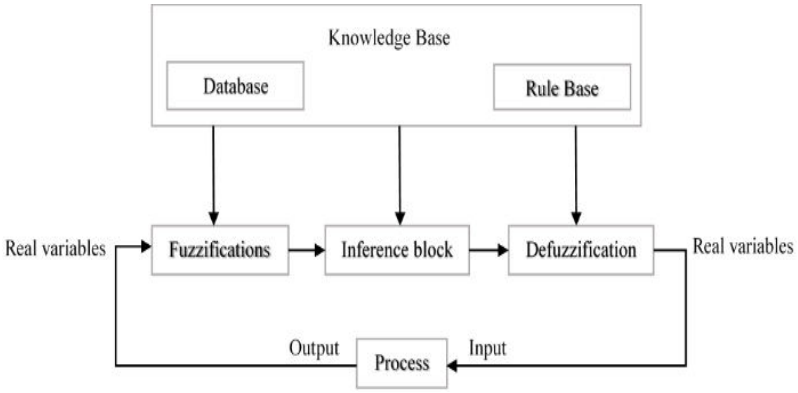

Fig.10: General block diagram of a fuzzy controller.

We begin by partitioning the various discourse universes imposed by the system into fuzzy subsets. Subsequently, we establish the rule base that will characterize the desired operation of the fuzzy variable. This step is known as fuzzification. The variables are then used in an inference mechanism, which generates and determines the fuzzy output variables through operations on membership functions.

11. MAXIMUM AND AVERAGE MAXIMUM METHOD

This method is notably simpler. The output value is chosen as the abscissa of the maximum value of the membership function. The principle of this approach lies in the choice of the abscissa associated with the maximum value of the resulting membership function. However, this method has a disadvantage. If the abscissa of the maximum value is confined between two values x_1 and x_2, any value within this range can be selected. Consequently, this method is not recommended for fuzzy logic control. This method generates a precise order by calculating the average of the values for which the membership is maximum. Its relation is given by:

$$u = \frac{\sum_{k=1}^{m} y_k}{m} \qquad (16)$$

Where m is the number of quantified values y_k for which the membership is maximal, [17].

12. MAMDANI CONTROLLER

In the following, we will consider the main type of fuzzy controller, the Mamdani type. This type of controller has been presented in a fuzzy application [18] and has the following general form for Nx inputs:

$$R_k: if\ x_1\ est\ A_{1k}\ \ and\ .et\ \ x_{Ns}\ is\ A_{Ns}\ then\ y\ est\ B_k$$

A block diagram of this type of controller is shown in Figure (11).

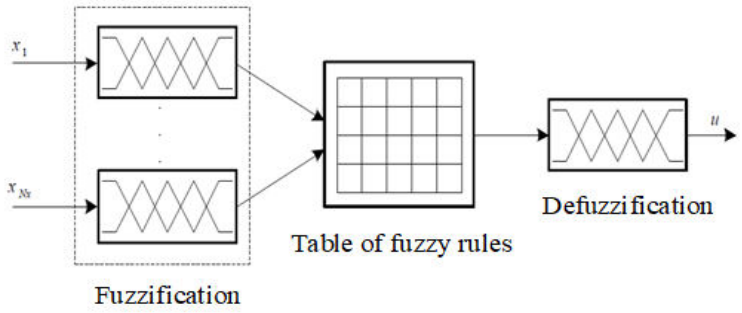

Fig.11: Mamdani controller

In fuzzy control systems, the input variables typically include the error (e), representing the difference between the variable to be controlled and its reference, and its rate of change (Δe). The "min" operator is utilized for the "and" operation and the "then" implication, while the "max" operator is employed for aggregating "or" rules. This inference mechanism is known as "min-max" type inference.

13. STRUCTURE OF THE FUZZY LOGIC CONTROLLER

The structure of the Fuzzy Logic Controller (FLC) proposed by Mamdani for a simple system with a single input and a single output is shown in Figure (12), which represents its internal structure.

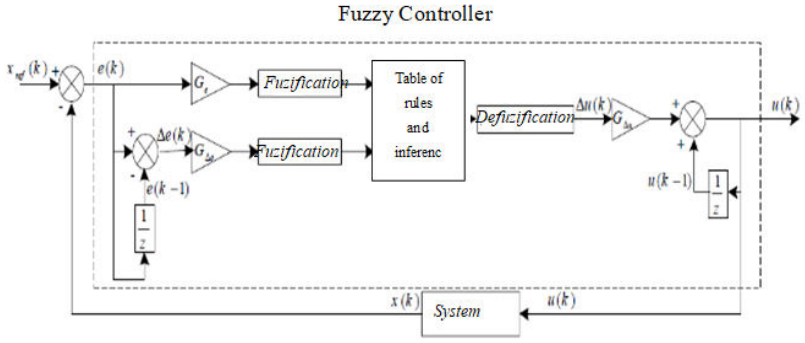

Fig.12: Mamdani's proposed fuzzy controller internal structure.

The two input quantities are discretized with a sampling period of T_e and normalized using normalization gains (G_e for error and $G_{\Delta e}$ for error variation). They are defined by the following expressions:

- The control error of the controlled variable is defined by the deviation:

$$e(k) = x^*(k) - x(k) \quad (17)$$

- The incremental variation of the adjustment error is defined by:

$$\Delta e(k) = e(k) - e(k-1) \quad (18)$$

The output of the fuzzy controller corresponds to the alteration in the output quantity. The updated value, adjusted at each sampling time, is defined by the following recurrent equation.

$$u(k) = u(k-1) + G_u \Delta_u(k) \quad (19)$$

Where G_u represents a denormalization gain for the output variable. These three gains enable global action on the control surface by either expanding or contracting the universe of discourse of the control variable.

14. MAIN CHARACTERISTICS OF THE FUZZY CONTROLLER

The main characteristics of the fuzzy controller used in this paper are as follows:

- Fuzzification with a continuous discourse universe [-1,1].
- Implication uses Mamdani's min-max inference.
- Seven fuzzy sets for the error and its variation defined by triangular membership functions.

Where: a=0.25, b=0.5, c=0.75; x ϵ [-1, 1]: takes either ef or Δef

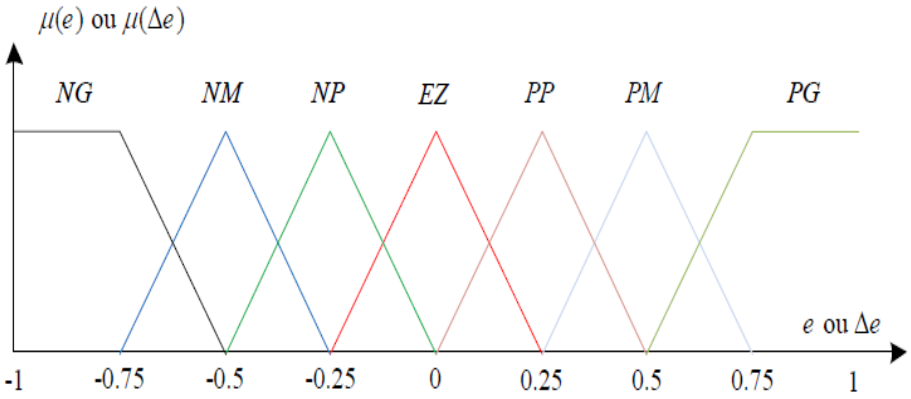

Fig.13: Distribution of selected membership functions.

Tab.2: Table of fuzzy rules.

		e						
		NG	NM	NP	EZ	PP	PM	PG
Δe	NG	NG	NG	NG	NG	NM	NP	EZ
	NM	NG	NM	NM	NM	NP	EZ	PP
	NP	NG	NM	NP	NP	EZ	PP	PP
	EZ	NM	NM	NP	EZ	PP	PM	PM
	PP	NP	NP	EZ	PP	PP	PM	PM
	PM	NP	EZ	PP	PM	PM	PM	PG
	PG	EZ	PP	PM	PG	PG	PG	PG

Table (2) shows the fuzzy rules used to design this controller.

The number of parameters to be set here is very large (7×7=49 parameters). Therefore, the controller is set in relation to the degrees of freedom associated with the membership functions of the input variables and the output variable, which have a global influence. This approach effectively restricts the number of variables in the controller.

The block diagram of the fuzzy control structure of a STATCOM is shown in Figure (14).

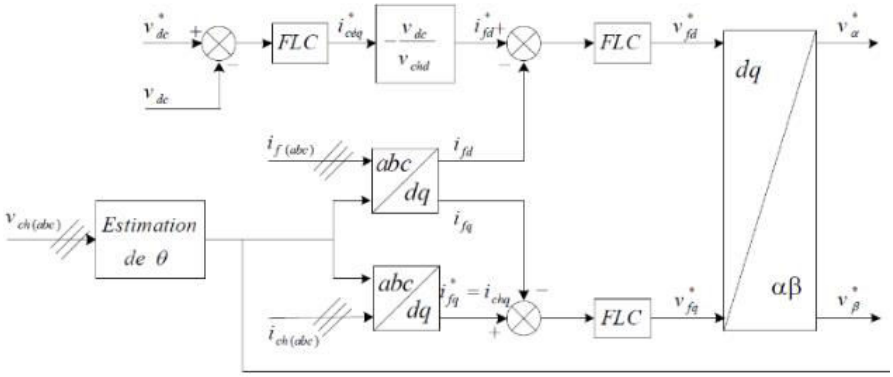

Fig.14: Controlling DC using fuzzy logic controller (FLC)

15. MODELLING THE NPC THREE-LEVEL INVERTER

Figure (15) illustrates the general structure of the three-level floating diode inverter, also known as the Neutral Point Clamped (NPC) inverter. This structure comprises two identical capacitors with a common midpoint denoted as "o", enabling the inverter to access an additional voltage level compared to the conventional two-level inverter [19].

Under normal operating conditions, the total voltage of the DC bus Vdc is evenly distributed across the two capacitors, resulting in a voltage of Vdc/2 at their terminals (this assumption is used in this section). The output is connected to a symmetrical three-phase star-connected load with an isolated neutral. The inverter consists of three arms: a, b, and c. Each arm comprises four fully controllable switches (Kx1, Kx2, Kx3, and Kx4, where x represents the arm index) connected in series, antiparallel with four main diodes to ensure the reversibility of currents in the load, along with two clamp diodes (Dx1 and Dx2) connected to the center of the DC bus.

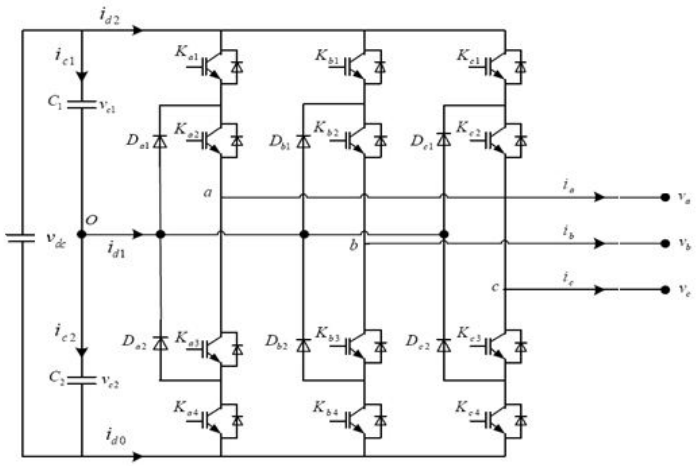

Fig.15: Power structure of the NPC three-phase three-level inverter.

16. DIFFERENT ELECTRICAL CONFIGURATIONS OF A THREE-LEVEL INVERTER ARM

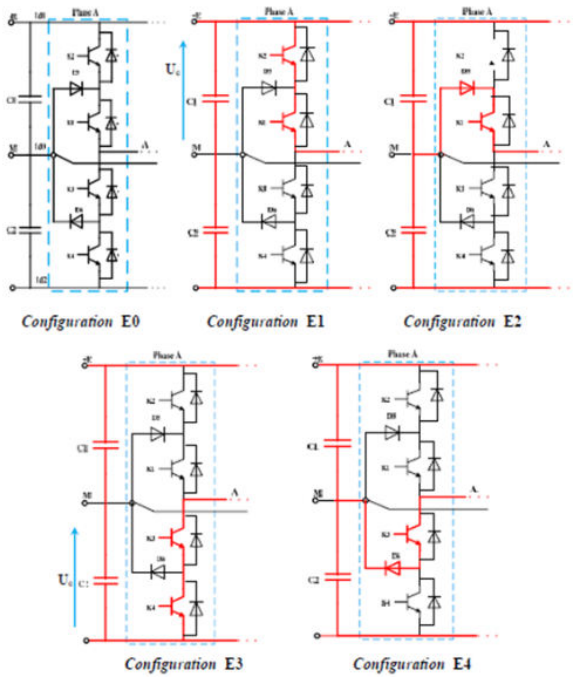

Fig.16: Various possible electrical configurations of a three-level inverter.

17. CONVENTIONAL PWM WITHOUT INJECTION OF THE THREE HARMONIC ON TWO UNIPOLAR CARRIERS

The control signals for one arm of the drive are determined by comparing two triangular carriers to a sinusoidal reference. The two carriers are defined by the following equations:

$$U_{p1} = \begin{cases} 2U_{p\,max}\frac{t}{T_p}\,; \text{pour } 0 \le t \le \frac{T_p}{2} \\ 2U_{p\,max}\left(-\frac{t}{T_p}+1\right); \text{pour } \frac{T_p}{2} \le t \le T_p \end{cases} \quad (20)$$

And:

$$U_{p2} = U_{p1} - U_{p\,max} \quad (21)$$

The algorithm used to implement this modulation technique is as follows:

$$\begin{cases} \text{if } (V_{réfk} > U_p)\ \&\ (V_{réfk} > U_{p2}) \text{then } S_{k1} = 1 \\ \text{else } S_{k1} = 0 \end{cases} \quad (22)$$

With: $S_{k2} = \overline{S}_{k1}$

18. SIMULATION RESULTS

The network consists of a 400 KV generator with a rated power of 3000 MVA, connected to the infinite network through the T-transformer and a 500 km transmission line modulated in π per 100 km.

The Tsh transformer is used to reduce the mains voltage (400 kV) to 34 kV (input voltage of the STATCOM shunt converter).

19. SIMULATION OF THE ELECTRICAL NETWORK WITHOUT COMPENSATION

In this section, we will present the behavior of the electrical network without a compensation system for different operating points, in relation to different values of transmitted active and reactive power:

- at t = 0s: a load of (30MW, 30MVRA) is applied,
- at t = 0.5s: the load is increased to (70MW, 50MVAR),
- at t =1.5s: the load is further increased to (95MW, 65MVAR),
- at t =2s: the load is reduced to (65MW, 30MVAR),
- at t = 2.5s: the load is reduced to (25MW, 15MVAR).

The aim of this section is to show the need for a compensation device.

To do this, we will show the results of simulations and in particular:

- Active and reactive power transmitted by the line.
- Line Currents and Voltages.

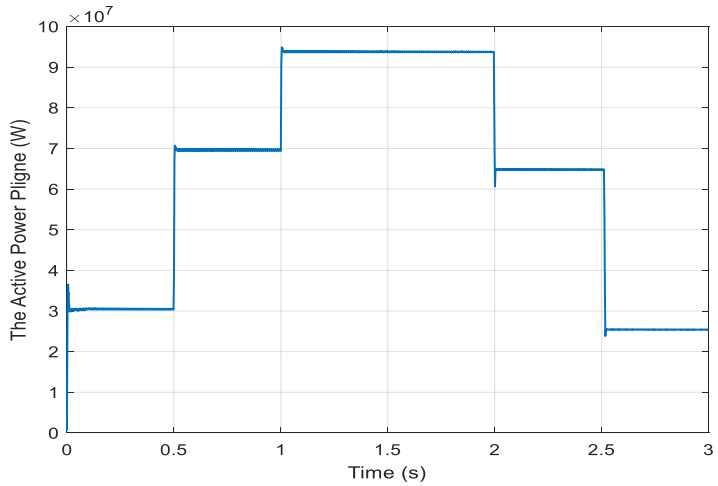

Fig.17: Active line power without compensation.

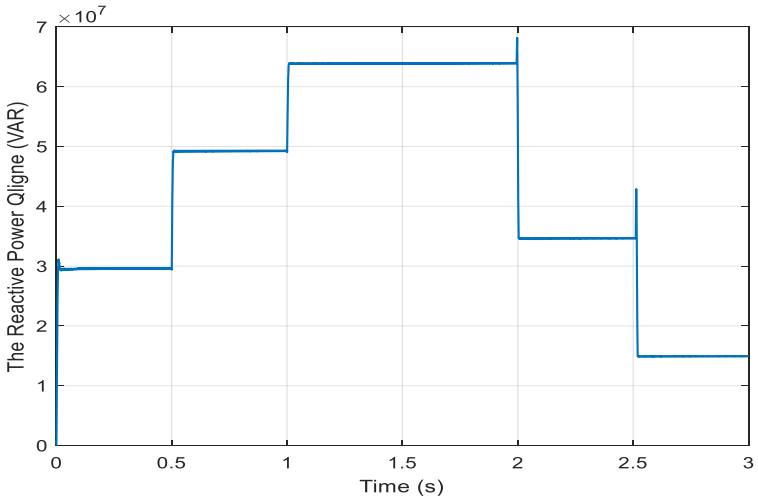

Fig.18: Reactive line power without compensation.

Figure (18) illustrates the variations in reactive power transmitted by the line, leading to in a non-uniform power factor. Consequently, this results in voltage drops and reduces the transmission capacity of the lines.

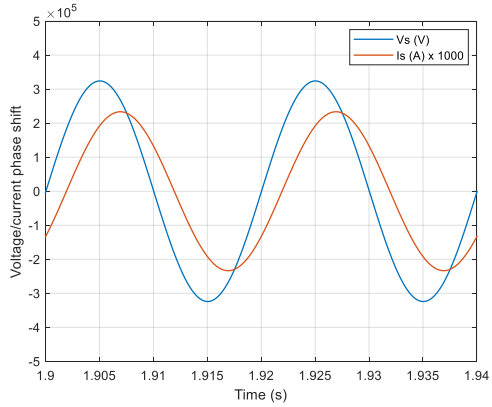

Fig.19: Phase shift between voltage and current source.

Figure (19) displays the phase shift between the source voltage and current. It is apparent that the source voltage is not in quadrature with the current, indicating variations in both active and reactive powers transmitted through the power line.

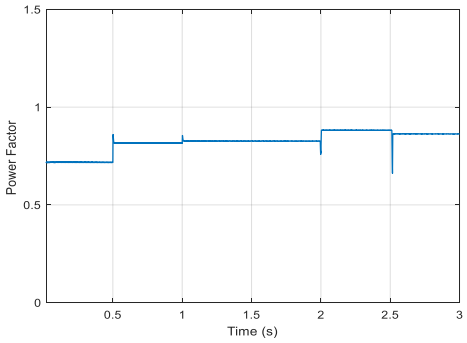

Fig.20: Power factor evolution.

20. SIMULATION OF THE ELECTRICAL NETWORK WITH COMPENSATION

This section highlights the significance of STATCOM in voltage control and reactive power compensation on power lines.

21. CHARACTERISTICS OF THE THREE-LEVEL INVERTER

The control signals for an inverter arm using a conventional PWM without injection of the third harmonic with two triangular unipolar carriers are determined by comparing two triangular carriers and a sinusoidal reference, as depicted in Figure (21).

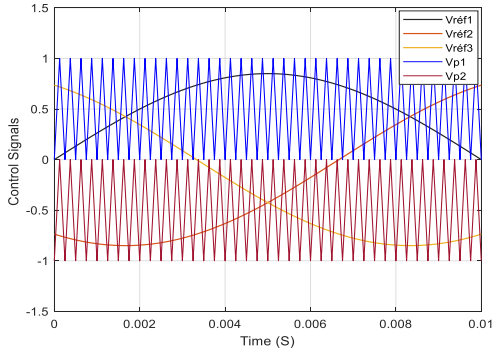

Fig.21: Principle of PWM control with two unipolar carriers.

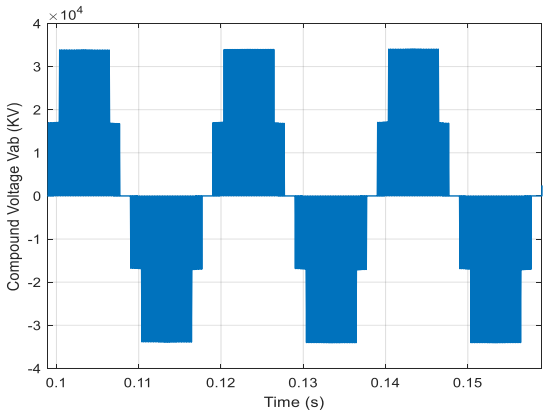

Fig.22: Compound voltage V_{ab} for r = 0.85 and m= 40

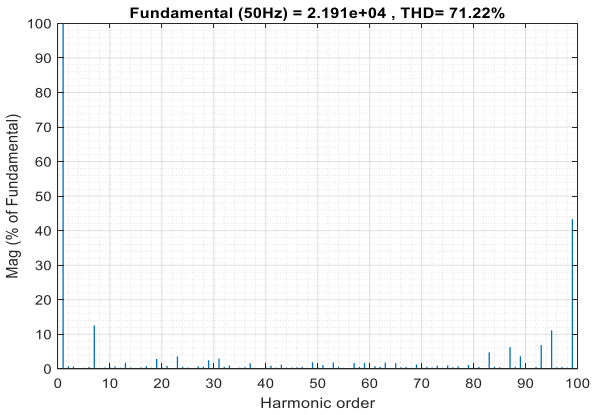

Fig.23: Harmonic spectrum of V_{ab}.

Figures (22) and (23) depict the composite voltage at the output of the STATCOM inverter. The four levels (E, E/2, -E/2, E) of the composite voltage can be seen, as well as the harmonic spectrum with a harmonic distortion rate of 71.22% for a regulation coefficient (r = 0.8) and a frequency modulation index (m = 40). It should be noted that for a conventional two-level inverter, the THD% is around double, which is an advantage of the chosen structure.

22. INFLUENCE OF SWITCHING FREQUENCY ON PHASE CURRENT

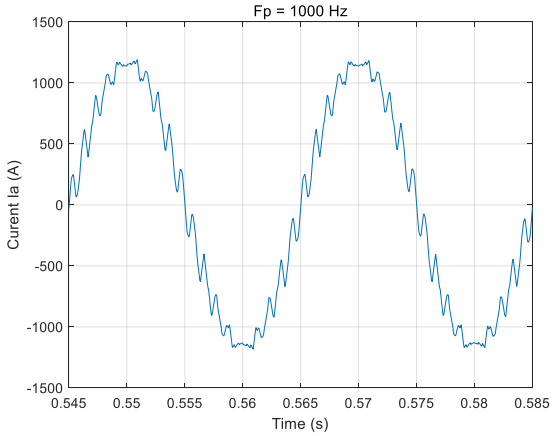

Fig.24: Ia current for Fp = 1000Hz.

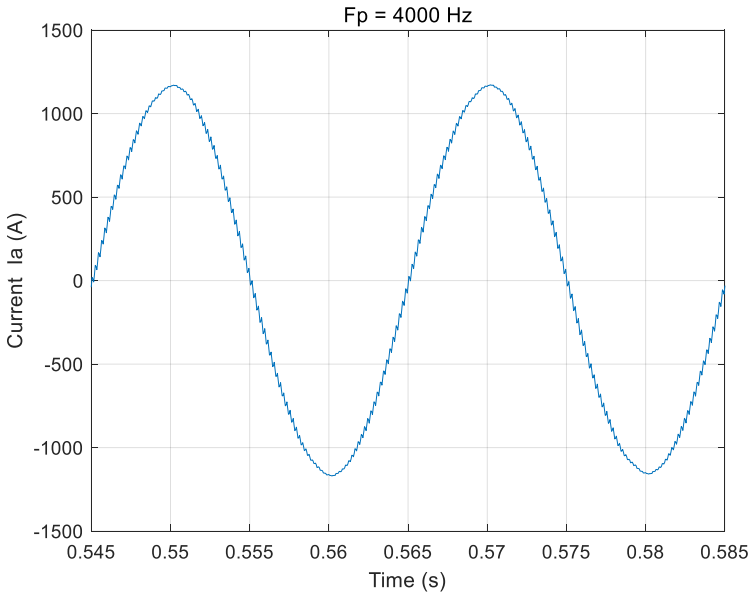

Fig.25: Ia current for F_p = 4000Hz

Figures (24) and (25) show the STATTCOM output current for two carrier frequencies 1 kHz and 4 kHz. It can be seen that as the frequency increases, the current ripple decreases and approaches a sinusoidal waveform. However, this frequency is constrained by both the specific application requirements and the technological limitations of the power switches in use.

23. RATE OF HARMONIC DISTORTION

Total Harmonic Distortion (THD) is a measure used to assess the deviation of a signal from a pure sinusoidal waveform.

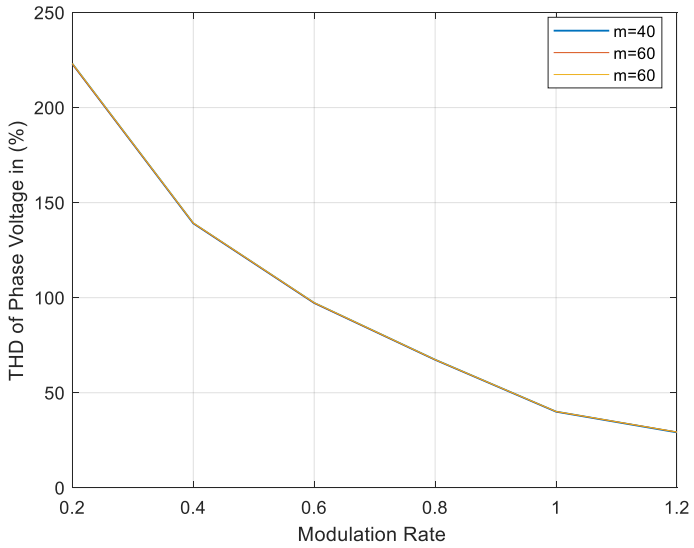

Fig.26: Phase voltage harmonic distortion rate.

Increasing the modulation index results in higher-frequency harmonics. However, as depicted in Figure (26), this increase does not affect the rate of harmonic distortion. Instead, the distortion rate decreases proportionally with the increase in modulation ratio.

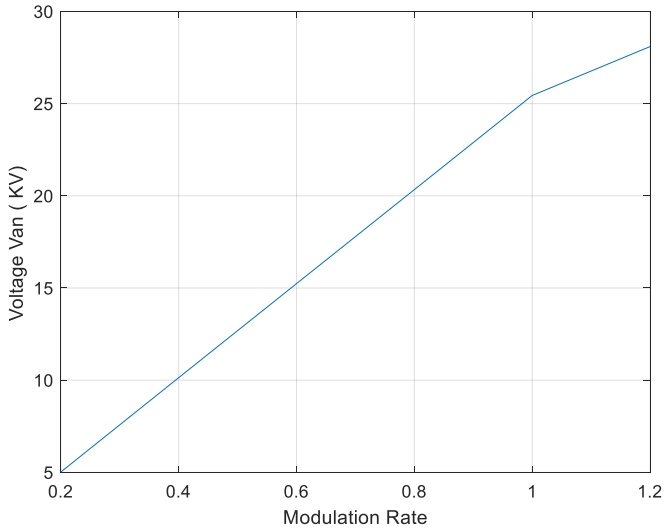

Fig.27: Setting characteristic for m=40.

From Figure (27) it can be seen that the modulation rate allows a linear adjustment of the fundamental amplitude in the range r ϵ [0, 1].

The use of three-level inverters for the application of STATCOM seems to be a rather interesting solution according to the following features.

- Increasing the modulation ratio (r = 0...1.2) reduces the THD.
- Increasing the modulation ratio r increases the number of harmonics in a family and at the same time reduces their amplitude.

The variation of the amplitude of the fundamental harmonic does not depend on the variation of the modulation index m.

24. CHARACTERISTICS OF THE SOURCE

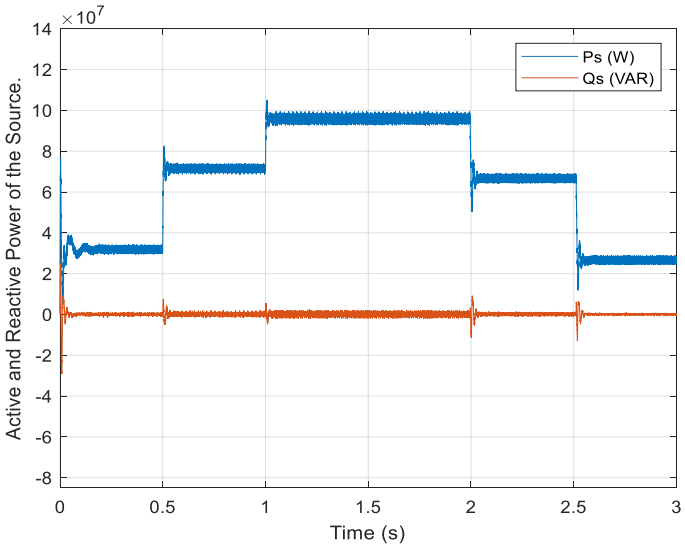

Fig.28: Source powers.

The complete compensation of reactive power in the lines demonstrates the efficiency of STATCOM.

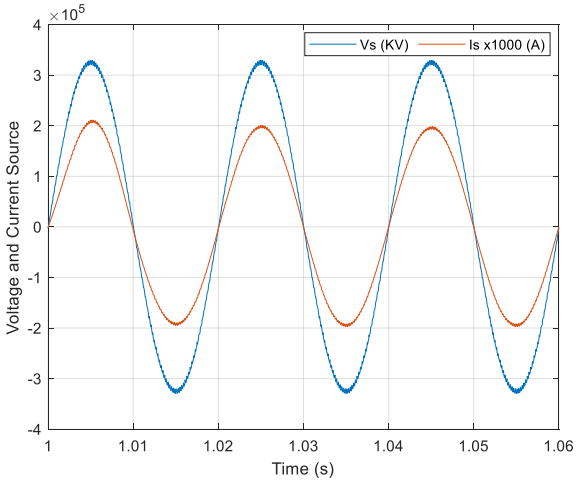

Fig.29: Phase shift between voltage and current source.

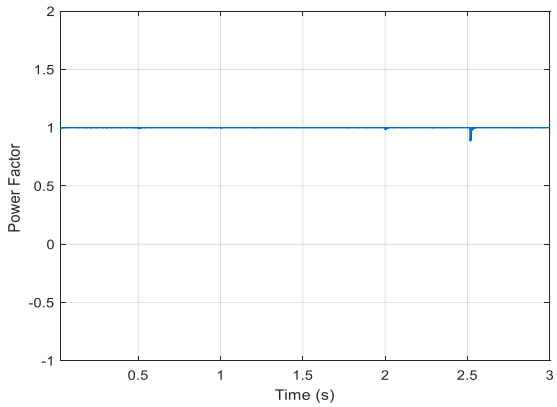

Fig.30: Power factor of the source.

Figure (29) illustrates that following compensation, the source voltage and current align in phase, indicating that the source operates with a unity power factor, Figure (30).

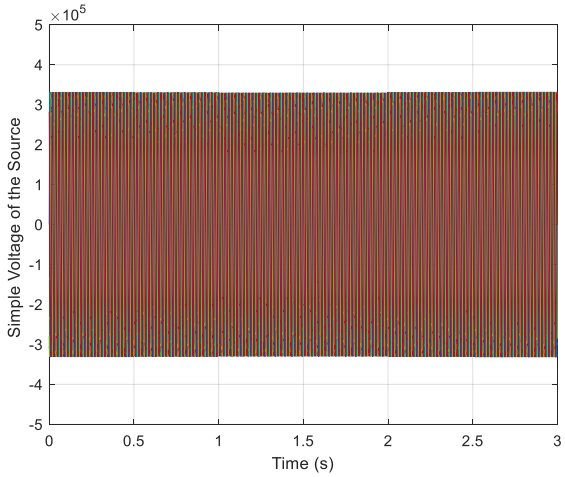

Fig.31: Simple source voltage.

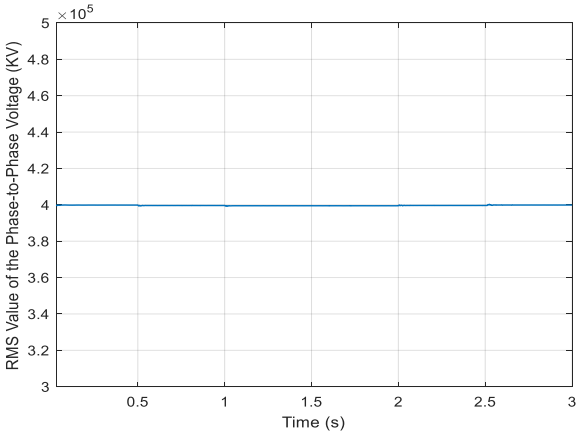

Fig.32: RMS composite value of the source.

Figures (31) and (32) show how STATCOM maintains voltage.

25. THE CHARACTERISTICS OF STATCOM

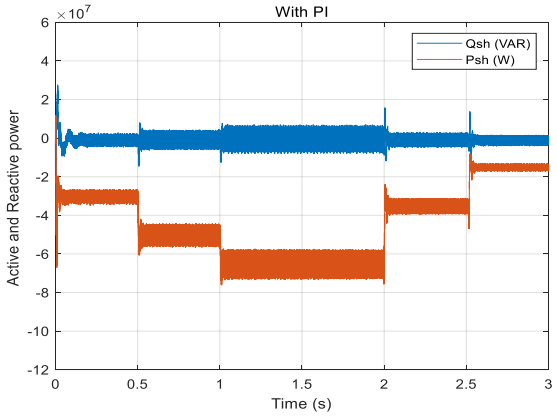

Fig.33: Power injected by STATCOM.

Figure (34) depicts that the STATCOM consumes minimal active power, which is justified by the losses in the inverter, filter and transformer. On the other hand, the STATCOM injects the required reactive power into the electrical system according to the reactive power variations of the loads.

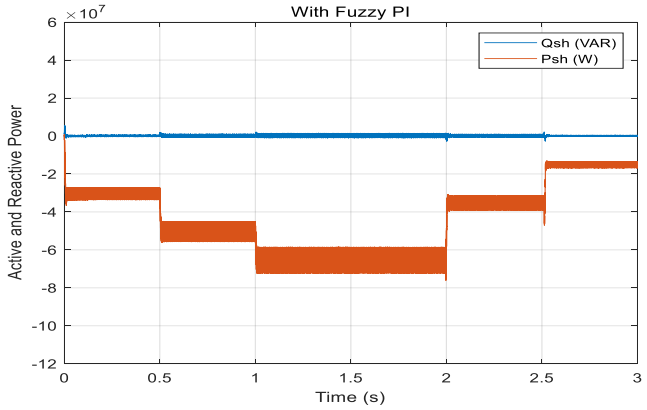

Fig.34: Active and reactive power injected by STATCOM.

Figure (34) illustrates a very good representation of the STATCOM performance:

- No start up oscillation.
- Low ripple.
- Very good noise rejection (load variation).

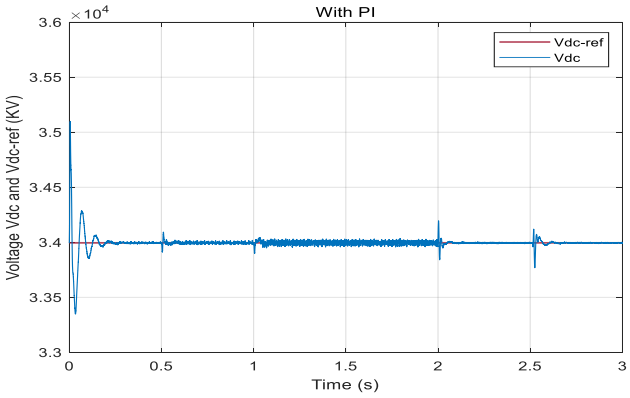

Fig.35: Voltage Vdc and Vdc-ref with PI regulator

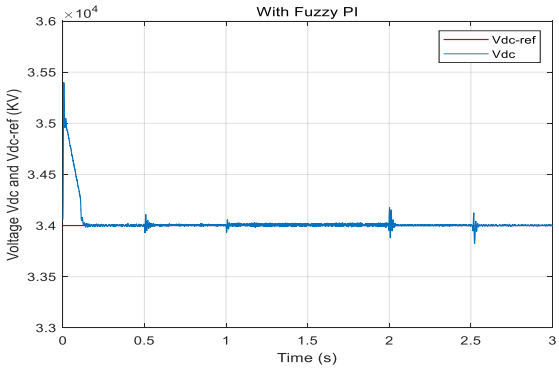

Fig.36: Voltage Vdc and Vdc-ref with FLC

As illustrated in Figure (36), it is evident that the voltage regulation block consistently demonstrates its effectiveness in maintaining a constant voltage across the global DC bus. The voltage undergoes a transient phase lasting less than 0.12 seconds as the load varies, before promptly returning to its reference value with zero static error.

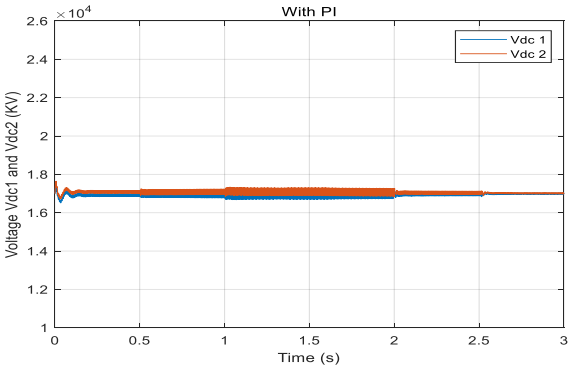

Fig.37: Voltage across the two capacitors with PI regulators

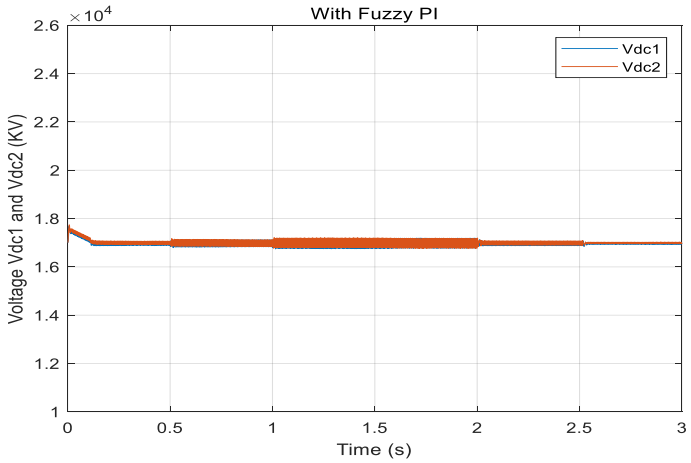

Fig.38: Voltage across the two capacitors with a fuzzy PI.

Figure (38) illustrates the stability and balance of the voltages across of the two DC bus capacitors.

Table (3), provides a comparative analysis between the PI and the fuzzy PI control strategies.

Tab.3: PI and FLC performances for Vdc control

Vdc	PI	Fuzzy PI
1st Overrun (%)	5.15	4.64
2nd Overrun (%)	1.91	0
3rd Overrun (%)	0.65	0
Ripple rate(%)	0.132	0.073
Response time(s)	0.2	0.122

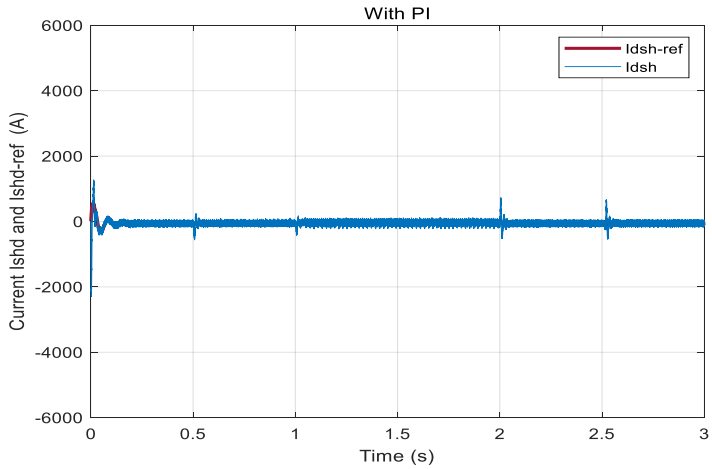

Fig.39: Active current and its reference injected by the STATCOM with PI regulators.

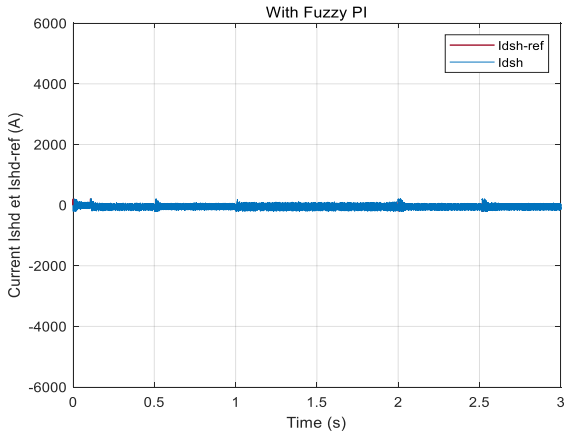

Fig.40: Active current and its reference injected by the STATCOM with FLC

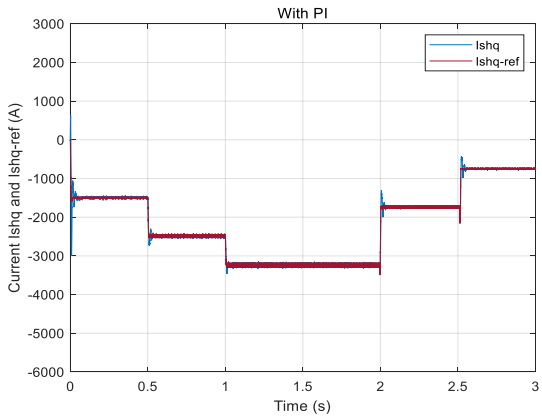

Fig.41: Reactive current and its reference injected by the STATCOM with PI.

Figures (42), (40) and (38) demonstrate the efficacy of the fuzzy controllers used, showcasing that the reactive current, active current and DC voltage follow their references with low overshoot and zero steady-state static error.

We are particularly interested in the reactive current (Iqsh) as it enables direct control of the injected reactive power.

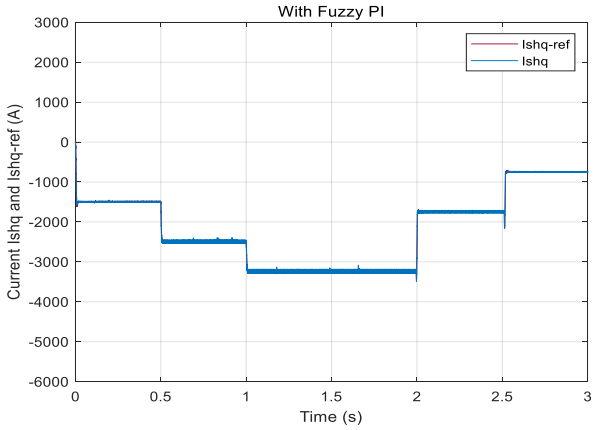

Fig.42: Reactive current and its reference injected by the STATCOM with FLC.

Table (4) presents a comparative study between PI and FLC control I_q current.

Tab.4: PI and fuzzy PI performance for I_q

	PI	FLC
1st Overrun (%)	1.20	1.01
2nd Overrun (%)	2.48	0
3rd Overrun (%)	2.05	0
Ripple rate(%)	2.64	0.71
Response time(s)	0.064	0.019

26. TRANSIENT REGIME WHEN STATCOM IS CONNECTED TO THE NETWORK

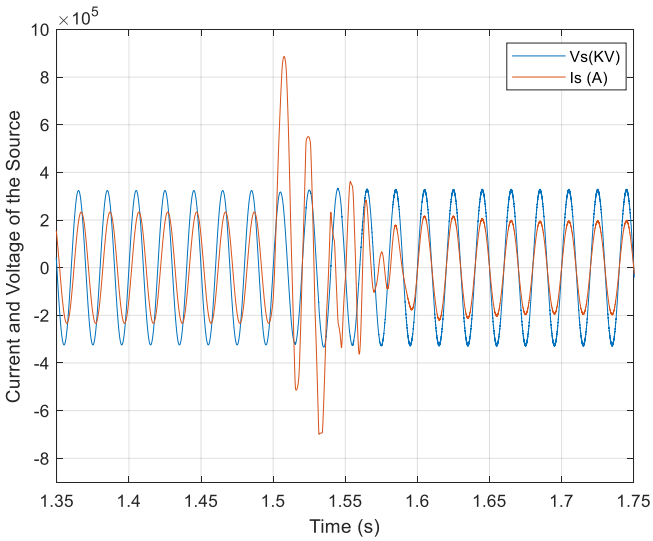

Fig.44: Current and Voltage Source in transient mode

Figure (43) depicts the evolution of the source voltage and current before and after compensation. It demonstrates that the power factor reaches unity (source current and voltage in phase) after four network periods, indicating the effectiveness of the chosen regulators.

27.CONCLUSION

Based on the simulation results obtained, we can conclude that the performance of the fuzzy logic controlled STATCOM is highly satisfactory in both steady state and transient conditions. This indicates that the fuzzy controller outperforms the conventional PI controller, especially in the transient regime. Notably, the fuzzy controller exhibits very rapid dynamic control in response to sudden load change and effectively functions as a disturbance damper.

28.REFERENCES

[1] N. Hingorani and L. Gyugyi, Understanding FACTS, Concepts and Technology of Flexible ac Transmission Systems. New York: IEEE Press, 2000.

[2] Z. Huang, Y. Ni, C.M. Shen, et al, "Application of Unified Power Flow Controller in Interconnected Power Systems - Modeling, Interface, Control Strategy, and Case Study", IEEE Trans. On Power Systems, vol. 15, No. 2, pp. 817-824, May 2000.

[3] D.K. Raju, B. S. Umre, M. P. Thakre, V. S. Kale, Mitigation of Subsynchronous oscillations with common controller based STACOM and SSSC, J. Electr. Eng. Elec-tron. Technol., 5, 1, pp. 735-744 (2016).

[4] Azra Hassanovic, Ali Feliachi, “Modelling and control of the Unified Power Flow Controller (UPFC)’’ these pour obtention du degree de master en science de l’ingénieur university de Morgantown, West Virginia, 2000.

[5] A. A. Nafeh, A. Heikal, R. A. El-Sehiemy, W. A. Salem, Intelligent fuzzy-based controllers for voltage stability enhancement of AC-DC micro-grid with DSTATCOM. Alexandria Engineering Journal, 61, 3, pp. 2260-2293 (2022).

[6] H. BÜHLER, Adjustment of Power Electronics Systems, Volume 3- Presse Polytechnique Romande 1999.

[7] Xia Jiang, "Operating Modes and Their Regulations of Voltage-sourced Converters Based FACTS Controllers", these de Doctorat de L'institut Polytechnique Troy New York, mars 2007.

[8] Pierre Bornard, Michel Pavard, "Interconnection and transmission networks : setting and operation", Technique de l'ingénieur traité Génie Electrique D 4090.

[9] Stéphane Gerbex. Metaheuristics Applied to the Optimal Placement of FACTS Devices in an Electrical Network", Doctoral thesis no. 2742 Ecole Polytechnique Fédérale de Lausanne (2003).

[10] M. Belghanem "Study and Analysis of a Three-Level Inverter used as a Static Reactive Energy Compensator". Magister's thesis, Mohamed Boudiaf University, Faculty of Electrical Engineering, Department of Electrical Engineering, July 1999.

[11] E.GH. Sahraki "Contribution of the UPFC to the Improvement of the Transient Stability of Electricity Networks", Doctoral Thesis University of Henri Poincaré, Nancy-I, October 13, 2003.

[12] K. Sreenivasachar "Unified Power Flow Controller: Modeling, Stability Analysis, Control Strategy, and Control System Design", These de Doctorate, Waterloo, Ontario, Canada, 2001.

[13] B.H. Chung, J-B Choo, X. Xy, B.P. Lam "Study of Operational Strategies of UPFC in KEPCO transmission System". IEEE, 2005.

[14] Nicolas Buyaut : Generalized "Control Study of Parallel Active Filters". Doctoral thesis, LANPES Doctoral School in Engineering Science 1999.

[15] K. Bouleriel: "Study and Simulation of a Control of the UPFC Unified Power Flow Electrical Controller", Master's thesis Mohamed Boudiaf University, Faculty of Electrical Engineering, Department of Electrical Engineering, July 2003.

[16] Nitus Voraphonpiput et Somchai Chatratana, "STATCOM Analysis and Controller Design for Power System Voltage Regulation", Transmission and Distribution Conference & Exhibition 2005 IEEE/PER.

[17] B. Robyns, F. Berthereau, J. P. Hauter and H. Buyse, "A Fuzzy-Logic-Based Multimodel Field Orientation in an Indirect FOC of Induction Motor", IEEE Transactions on Power Electronics, Vol. 47, No. 2, April 2000, pp. 380-388.

[18] E. Acha, V.G. Agelidis, O. Anaya- Lara and T. J. Miller "Power Electronic Control in Electrical Systems" liver, Newnes: Oxford, Aukland, Boston, Johannesburg, Melbourne, New Delhi. First Published 2002.

[19] L. Liming, Zhu. Pengcheng, Y. kang, J. Chen "Dsign and Dynamic Performance Analysis of a Unified Power Flow Controller", IEEE Transaction, 0-7803-9252-3. 2005.

29.AUTHORS INFORMATION

Leila Boukarana, She obtained a Magister degree in Electrical Engineering - Electrical Networks from the Faculty of Technology at the University of Batna 2, Algeria, in 2016.

She is a Doctoral Student at the University of Boumerdes, and a member of the LREEI Laboratory (Laboratoire de Recherche sur l'Electrification des Entreprises Industrielle) at the Faculty of Hydrocarbons and Chemistry.

Fellag Sid Ali Currently Professor at Boumedes University (Algeria) and, Director of Research Laboratory LIST (Ingenierie of Systems and Telecommunications) at Faculty of Technology. Got his PHD from Tashkent Polytechnical Institut in 2000 in the topic of Automation of Electro Technical Complexes-Long belt conveyers. Joined Algerian University since 2000- up today. Worked on Multirotor Systems, wind Energy, Solar Energy and Recently Working in Biomedical Engineering field Supervising a PHD thesis on ECG Signal Detection and Classification.

Idir Habi, Professor at the University of Boumerdes He obtained his Doctorate from the Institut National Polytechnique de Loraine INPL Nancy France 1987 in Electrical Engineering with a computer option. Joined the Algerian University in 1987, and is currently Director of the LREEI Research Laboratory (Laboratoire de Recherche sur l'Electrification des Entreprises Industrielle) at the Faculty of Hydrocarbons and Chemistry, and a Member of the Scientific Advisory board of the Automation and Electrification of Industrial

Processes department at the University of Boumerdes. He has worked on industrial electrical technology, teaching methods and introduction to scientific research, and computer networks.